

Interaction of strongly chirped pulses with two-level atoms

S. Ibáñez,¹ A. Peralta Conde,¹ D. Guéry-Odelin,² and J. G. Muga¹

¹*Departamento de Química Física, Universidad del País Vasco - Euskal Herriko Unibertsitatea, Apdo. 644, Bilbao, Spain*

²*Laboratoire Collisions Agrégats Réactivité, CNRS UMR 5589, IRSAMC, Université Paul Sabatier, 118 Route de Narbonne, F-31062 Toulouse CEDEX 4, France*

(Received 26 May 2011; published 29 July 2011)

We study the effect of ultrachirped pulses on the population inversion of two-level atoms. Ultrachirped pulses are defined as those for which the frequency chirp is of the order of the transition frequency of the two-level atom. When the chirp is large enough, the resonance may be crossed twice, for positive and negative frequencies. In fact the decomposition of the field into amplitude and phase factors, and the corresponding definition of the instantaneous frequency, are not unique. The interaction pictures for different decomposition are strictly equivalent, but only as long as approximations are not applied. The domain of validity of the formal rotating wave approximation is dramatically enhanced by a suitable choice, the so-called analytic signal representation.

DOI: [10.1103/PhysRevA.84.013428](https://doi.org/10.1103/PhysRevA.84.013428)

PACS number(s): 33.40.+f, 32.80.Qk, 42.50.-p

I. INTRODUCTION

Taking the parameters of a system to extreme values beyond their standard domain is a common and fruitful exercise in physics. It frequently discloses different regimes, properties, or qualitative changes in the system behavior. Appropriate modifications in the theoretical or experimental treatments or plainly new tools may also be required, and often the new physics found leads to unexpected applications. Examples of much current interest in atomic, molecular, and optical science are ultracold temperatures, or ultrashort and ultrastrong field-matter interactions. In this paper we want to put forward and examine the limit of ultrachirped pulses. By an “ultrachirped pulse” we mean one where the instantaneous frequency change is of the order of the transition frequency of a two-level (actual or artificial) atom. We shall describe in particular linearly chirped pulses that excite the resonance twice, at positive and negative instantaneous frequencies, as derived from the common decomposition of the field into amplitude and phase factors.

Except for monochromatic, constant-intensity fields, the choice of amplitude and phase to describe the field is not unique, and it affects the definition of the Rabi frequency $\Omega_R(t)$, instantaneous frequency $\omega(t)$, and detuning $\Delta(t)$. This leads to different interaction pictures and different accuracies for the corresponding rotating wave approximations (RWA), a widespread simplification to treat radiation-matter interaction neglecting rapidly oscillating terms. Its validity has been analyzed for different applications [1], and the deviations from exact results are currently of much interest due to the increasing ability to manipulate interaction parameter values in different physical settings, and to produce strong couplings and/or ultrashort pulses. We demonstrate that a particular amplitude-phase partition, the one provided by the analytic signal theory, enhances significantly the domain of validity of the RWA with respect to the most common (quadrature model) partition. To make the paper self-contained we shall first review briefly in the following subsections the elements of interaction pictures for time dependent parameters and of analytic signal theory. Section II is devoted to the population inversion induced by the linearly ultrachirped Gaussian pulse.

A. General formulation of intermediate pictures

Interaction pictures (IP) or “representations” [2], intermediate between the Schrödinger and Heisenberg pictures, may be most generally formulated in terms of a unitary operator $U_0(t)$ [2], which defines, from the Schrödinger picture state $\psi_S(t)$, the IP state $\psi_I(t) = U_0^\dagger(t)\psi_S(t)$. $\psi_I(t)$ evolves according to the dynamical equation $i\hbar\partial_t\psi_I(t) = H_I(t)\psi_I(t)$, where

$$H_I(t) = U_0^\dagger(t)H'(t)U_0(t), \quad (1)$$

$$H'(t) = H(t) - H_0(t), \quad (2)$$

$$H_0(t) = i\hbar\dot{U}_0U_0^\dagger. \quad (3)$$

$H(t)$ is the Schrödinger picture Hamiltonian and the dot denotes derivative with respect to t . In this general formulation the primary object is the unitary operator $U_0(t)$, and $H_0(t)$ is “derived” as the Hamiltonian for which $U_0(t)$ is an evolution operator. In many textbooks the emphasis is the opposite: the starting point is a splitting of the Hamiltonian $H(t) = H_0(t) + H'(t)$, and then $U_0(t)$ is defined as the evolution operator of $H_0(t)$ [3]. Quite frequently $H_0(t)$ is time-independent and $U_0(t) = e^{-iH_0t/\hbar}$, as in typical applications of time-dependent perturbation theory, but we stress that this is only a particular case and by no means necessary.

B. Interaction pictures for a two-level atom

We shall assume a semiclassical description of the interaction between a laser electric field linearly polarized in x direction, $\mathbf{E}(t) = E(t)\hat{x}$, and a two-level atom. Hereafter we shall refer to $E(t) = E_0(t)\cos[\theta(t)]$ as “the field.” In the electric dipole approximation, and for the general case where the transition frequency $\omega_0(t)$ may depend on time, the exact Hamiltonian of the atom in the Schrödinger picture is

$$H_e(t) = \frac{\hbar\omega_0(t)}{2} [|2\rangle\langle 2| - |1\rangle\langle 1|] + \frac{\hbar\Omega_R(t)}{2} [(|2\rangle\langle 1| + |1\rangle\langle 2|)(e^{i\theta(t)} + e^{-i\theta(t)})], \quad (4)$$

where $|1\rangle$ is the ground state and $|2\rangle$ the excited state of the isolated two-level atom, $\theta(t) = \int_0^t \omega(t')dt'$, and $\omega(t) = \dot{\theta}(t)$ is the instantaneous frequency. $\Omega_R = \Omega_R(t) = cE_0(t)$ is the Rabi

frequency with c a real constant, the component of the dipole moment in the polarization direction divided by \hbar . Note that the definitions of $\omega(t)$ and Ω_R are not unique, as emphasized below. It is usually convenient to write the phase as $\theta(t) = \omega_L t + \varphi(t)$, taking ω_L as a constant, the carrier frequency, so that $\omega(t) = \omega_L + \dot{\varphi}(t)$.

The laser-adapted interaction picture, also called in this context rotating frame, based on defining

$$H_0(t) = H_L(t) = \frac{\hbar\omega(t)}{2}(|2\rangle\langle 2| - |1\rangle\langle 1|) \quad (5)$$

and

$$U_0(t) = e^{-i\int_0^t H_L(t')dt'/\hbar} = e^{-i\theta(t)/2}|2\rangle\langle 2| + e^{i\theta(t)/2}|1\rangle\langle 1|, \quad (6)$$

produces the IP Hamiltonian¹

$$H_I(t) = \frac{\hbar}{2} \begin{pmatrix} -\Delta(t) & (1 + e^{-2i\theta(t)})\Omega_R(t) \\ (1 + e^{2i\theta(t)})\Omega_R(t) & \Delta(t) \end{pmatrix}, \quad (7)$$

where we use the vector basis $|1\rangle = \begin{pmatrix} 1 \\ 0 \end{pmatrix}$, $|2\rangle = \begin{pmatrix} 0 \\ 1 \end{pmatrix}$, and

$$\Delta(t) \equiv \omega_0(t) - \omega(t) \quad (8)$$

is the detuning between the transition frequency and the instantaneous frequency. If $\omega_0(t)$ does not depend on time and $\omega_0 = \omega_L$, as we shall assume hereafter,

$$\Delta(t) = -\dot{\varphi}(t). \quad (9)$$

Applying now a RWA to get rid of the counter-rotating terms we end up with

$$H_{I,RWA}(t) = \frac{\hbar}{2} \begin{pmatrix} -\Delta(t) & \Omega_R(t) \\ \Omega_R(t) & \Delta(t) \end{pmatrix}. \quad (10)$$

This is a ‘‘formal’’ RWA applied blindly at this point, without analyzing the frequency content of the neglected phase factors $e^{\pm 2i\theta}$, to be distinguished from a more accurate treatment in which the phase factor is Fourier analyzed and filtered. The term ‘‘RWA’’ refers here to this crude, formal approach which, as we shall see, will be valid or not depending on the field partition chosen.

C. Phase and instantaneous frequency of a signal

We summarize here some relevant elements of signal theory [5]. A general real signal can be written in the form

$$s(t) = a(t) \cos \theta(t), \quad (11)$$

where $a(t)$ is the amplitude and $\theta(t)$ the phase. This decomposition of $s(t)$, however, is not unique. In other words, we may find different amplitude and phase functions a' and θ' satisfying $s(t) = a'(t) \cos \theta'(t)$.

It is customary to define a corresponding complex signal,

$$Z(t) = A(t)e^{i\Theta(t)}, \quad (12)$$

with real part $s(t)$,

$$Z(t) = s(t) + i s_i(t), \quad (13)$$

and imaginary part $s_i(t)$ defined in different ways. For a given complex signal the instantaneous frequency is defined as the derivative of the phase, $\omega(t) = \dot{\Theta}(t)$, so it depends on the imaginary part chosen.

Moments of the signal may be defined as $\langle t^n \rangle = \int s^2 t^n dt / \int s^2 dt$, and the variance is $\sigma_t^2 = \langle t^2 \rangle - \langle t \rangle^2$. This extends to complex signals as well changing $s^2 \rightarrow |Z|^2$. In frequency space, spectral moments are defined similarly in terms of the spectrum of $s(t)$,

$$S(\omega) = \frac{1}{\sqrt{2\pi}} \int_{-\infty}^{\infty} s(t) e^{-i\omega t} dt, \quad (14)$$

and the bandwidth σ_ω is defined as the root of the variance. For a real signal $S(-\omega) = S^*(\omega)$, and $|S(\omega)|^2$ is symmetric about the origin, so $\langle \omega \rangle = 0$. It is also possible to extend the spectrum concept to the complex signal, or to parts of it, and break this symmetry.

1. The quadrature signal

From Eq. (11), it is natural to write the complex signal as

$$s_q(t) = a(t)e^{i\theta(t)}, \quad (15)$$

which is called the quadrature (model) signal. As Eq. (11) is not unique, the quadrature signal is not unique either. $S_q(\omega)$ is the corresponding spectrum.

2. The analytic signal

The analytic signal is a peculiar complex signal chosen as

$$s_a(t) = \frac{2}{\sqrt{2\pi}} \int_0^\infty S(\omega) e^{i\omega t} d\omega. \quad (16)$$

The imaginary part $s_{a,i}(t)$ is the Hilbert transform of the real signal $s(t)$. $s_a(t)$ can also be written in terms of its amplitude $A_a(t) = (s^2 + s_{a,i}^2)^{1/2}$ and its polar phase $\theta_a(t)$ as

$$s_a(t) = A_a(t)e^{i\theta_a(t)}. \quad (17)$$

One of the advantages of the analytic signal is that it puts the low frequencies in the amplitude and the high frequencies in the phase factor $e^{i\theta_a(t)}$ [5]. If the spectrum of the amplitude is of finite support, the support of the spectrum of the phase factor does not overlap and this makes the pair $[A_a(t), \theta_a(t)]$ unique. The spectrum of $s_a(t)$ is $S_a(\omega) = 2S(\omega) = S_q(\omega) + S_q^*(-\omega)$ if $\omega > 0$ and zero otherwise.

The maximum possible deviation of a quadrature signal from the analytic signal, at time t , is given by

$$|s_a(t) - s_q(t)| \leq \frac{2}{\sqrt{2\pi}} \int_{-\infty}^0 |S_q(\omega)| d\omega. \quad (18)$$

Another criterion of closeness is that

$$\int |s_a(t) - s_q(t)|^2 dt = 2 \int_{-\infty}^0 |S_q(\omega)|^2 d\omega \quad (19)$$

should be small, i.e., the spectrum of the quadrature signal should be predominantly in the positive frequency domain [5].

¹This was termed, with a different notation ‘‘quasi-interaction picture’’ in [4]. In fact, according to the definition of IP given above, it is a perfectly canonical one.

II. RWA WITH THE QUADRATURE AND THE ANALYTIC SIGNALS FOR A LINEARLY CHIRPED GAUSSIAN PULSE

We consider now an electric field with a Gaussian envelope and a linear chirp,

$$E(t) = \mathcal{E}_0 e^{-at^2} \cos(\omega_L t + bt^2), \quad (20)$$

as the real signal, where $E_0(t) = \mathcal{E}_0 e^{-at^2}$ is its amplitude with maximum value \mathcal{E}_0 , a is a positive constant, b a real chirp parameter, and ω_L is the carrier frequency. Not to restrict the numerical examples to a particular system or region of the spectrum, we shall from now on use dimensionless variables. We define $\tilde{t} = a^{1/2}t$, $\tilde{\omega} = \omega/a^{1/2}$, and apply the same scaling to all times and frequencies. Similarly, $\tilde{b} = b/a$. From the definition of the dimensionless Rabi frequency, $\tilde{\Omega}_R = \Omega_R/a^{1/2}$, the dimensionless amplitude of the field is $\tilde{E}_0 = \mathcal{E}_0 e^{-\tilde{t}^2}$, where $\tilde{\mathcal{E}}_0 = c\mathcal{E}_0/a^{1/2}$. Dimensionless Hamiltonians are defined as $\tilde{H} = H/(a^{1/2}\hbar)$. To avoid a heavy notation we finally drop all the tildes hereafter. The dimensionless version of Eq. (20) is thus

$$E(t) = \mathcal{E}_0 e^{-t^2} \cos(\omega_L t + bt^2), \quad (21)$$

see an example in Fig. 1.

The corresponding quadrature model signal is

$$E_q(t) = \mathcal{E}_0 e^{-t^2} e^{i(\omega_L t + bt^2)}, \quad (22)$$

with amplitude $E_{0q}(t) = \mathcal{E}_0 e^{-t^2}$, phase $\theta_q(t) = \omega_L t + bt^2$, and instantaneous frequency $\omega_q(t) = \omega_L + 2bt$ corresponding to a linear chirp. For this quadrature signal $\langle t \rangle = 0$ and $\sigma_{tq}^2 = \langle t^2 \rangle = \int |E_q(t)|^2 t^2 dt / \int |E_q(t)|^2 dt = 1/4$.

The dimensionless interaction picture Hamiltonian in the rotating wave approximation, Eq. (10), becomes

$$H_{I,RWA,q}(t) = \frac{1}{2} \begin{pmatrix} -\Delta_q(t) & \Omega_{Rq}(t) \\ \Omega_{Rq}(t) & \Delta_q(t) \end{pmatrix}, \quad (23)$$

where $\Delta_q(t) = -2bt$ if $\omega_0 = \omega_L$.

The analytic model signal provides instead the complex field $E_a(t)$ according to Eqs. (16) and (17),

$$E_a(t) = E_{0a}(t) e^{i\theta_a(t)}. \quad (24)$$

The corresponding interaction picture is different from the one using the quadrature model, and the RWA Hamiltonian, Eq. (10), becomes

$$H_{I,RWA,a}(t) = \frac{1}{2} \begin{pmatrix} -\Delta_a(t) & \Omega_{Ra}(t) \\ \Omega_{Ra}(t) & \Delta_a(t) \end{pmatrix}, \quad (25)$$

where $\Delta_a(t) = \omega_0(t) - \omega_a(t)$, with $\omega_a(t) = \dot{\theta}_a(t)$.

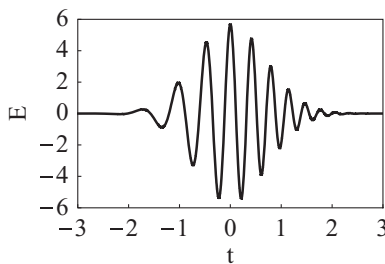


FIG. 1. Linearly chirped Gaussian pulse. Parameters: $b = 2$, $\mathcal{E}_0 = 4\sqrt{2}$, and $\omega_L = 10\sqrt{2}$.

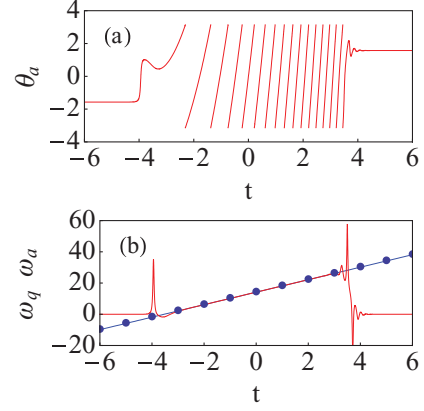


FIG. 2. (Color online) (a) Phase of the analytic signal $\theta_a(t)$ from $-\pi$ to π . (b) The instantaneous frequency $\omega_a(t)$ (solid red line) following the linear form of $\omega_q(t) = \omega_L + 2bt$ (blue line with dots) in the central interval and tending asymptotically to zero. Parameters: $b = 2$, $\mathcal{E}_0 = 4\sqrt{2}$, and $\omega_L = 10\sqrt{2}$.

To calculate $E_a(t)$ we may use the relation [5]

$$E(\omega) = \frac{1}{2} [E_q(\omega) + E_q^*(-\omega)], \quad (26)$$

where $E(\omega)$ is the spectrum of $E(t)$, and

$$E_q(\omega) = \frac{1}{\sqrt{2\pi}} \int_{-\infty}^{\infty} E_q(t) e^{-i\omega t} dt = \frac{\mathcal{E}_0 e^{-(\omega - \omega_L)^2/4(1-ib)}}{\sqrt{2(1-ib)}}. \quad (27)$$

Then, from Eq. (16),

$$E_a(t) = \frac{\mathcal{E}_0}{2} [e^{-\omega_L^2/4(1-ib)} w(z) + e^{-\omega_L^2/4(1+ib)} w(z^*)], \quad (28)$$

where $z = z(t) = t\sqrt{1-ib} - i\omega_L/(2\sqrt{1-ib})$ and $w(z) = e^{-z^2} \text{erfc}(-iz)$ is the Faddeyeva or w function [6,7]. One can verify that the real part of $E_a(t)$ is equal to $E(t)$, the amplitude and phase being now defined as $|E_a(t)|$ and $\text{Im}[\ln E_a(t)]$, respectively.

From Eq. (19) [5], and for our Gaussian electric field, $E_q(t) \sim E_a(t)$, at least in the central part of the pulse, for

$$\omega_L \gg \sqrt{2}\sigma_{\omega q}, \quad (29)$$

where $\sigma_{\omega q} = \sqrt{1+b^2}$ is the bandwidth of $E_q(t)$.

We have defined $\theta_q(t) = \omega_L t + bt^2$ to have a linear chirp, but $\theta_a(t)$ will have in principle a different form. When $E_a(t) \sim E_q(t)$ in a central interval, $\theta_a(t)$ follows the quadratic form of $\theta_q(t)$ there, but it becomes constant well before and after, see Fig. 2(a). The ‘‘parabola’’ is in fact cut into pieces corresponding to the principal branch of the logarithm, from $-\pi$ to π . Similarly, Fig. 2(b) shows that the instantaneous frequency $\omega_a(t)$ follows the linear form of $\omega_q(t) = \omega_L + 2bt$ in the central interval but it tends asymptotically to zero. The details of the transition are discussed in the Appendix.

A. Population inversion

If the dynamics is performed exactly, different amplitude and phase splittings of the field produce the same results. Only the real field matters, and the interaction pictures, although different, are all equivalent since they lead to the same

Schrödinger dynamics and to the same populations. Applying the RWA gives, however, different results.

Considering that the atom is initially in the ground state, we have solved numerically (with MATHEMATICA NDSolve) the system of two coupled differential equations for the wave function amplitudes $c_1(t), c_2(t)$, $|\psi\rangle = c_1(t)|1\rangle + c_2(t)|2\rangle$, i.e., generically we solve $i\hbar\partial_t|\psi\rangle = \mathcal{H}|\psi\rangle$, where \mathcal{H} may be the exact Hamiltonian, Eq. (7), or the approximate ones in Eqs. (23) and (25), using the boundary conditions $c_1(0) = 1$, $c_2(0) = 0$.

The validity of the RWA is usually discussed for time-independent frequencies and linked to assuming first the weak-coupling condition [8,9],

$$\omega_0 \gg \Omega_R(t), \quad (30)$$

and then a quasiresonance condition $|\Delta|/\omega_0 \ll 1$. This later condition is clearly violated out of resonance for ultrachirped pulses. Nevertheless, if the condition in Eq. (30) is satisfied and ω_L is also large enough to satisfy the closeness condition in Eq. (29), the populations of the excited state $P_2(t) = |c_2(t)|^2$ driven by the two approximate Hamiltonians are equal to each other and to the population driven by the exact Hamiltonian. When Eq. (29) is not satisfied, however, the populations $P_2(t)$ driven by these approximate Hamiltonians are different and the range of validity of the RWA is much wider for the analytic signal than for the quadrature, as we shall see.

The parameters of the system, considering that $\omega_0(t) = \omega_L$, are \mathcal{E}_0 , ω_L , and b . For the values $\mathcal{E}_0 = 200$, $b = 3500$, and $\omega_L = 20000$, see Fig. 3, the population is fully transferred to the excited state according to the exact dynamics. We then decrease ω_L up to 700. Figures 3–5 show that in this range of carrier frequencies, the population of the excited state $P_2(t)$ with the analytic signal RWA follows the exact results, while the quadrature RWA fails. At $\omega_L = 700$, see Fig. 5, the quadrature RWA model predicts full inversion, whereas the analytic RWA model and the exact results give a complete population return.

This behavior shows up that the condition in Eq. (30) for the quadrature RWA is much more strict than for the analytic signal RWA. To reach the agreement between the quadrature RWA and the exact dynamics we have to set $\omega_L = 20000$, 100 times greater than the maximum of $\Omega_{Rq}(t)$, $\Omega_{Rq}(0) = 200$, whereas the analytic signal RWA still follows the exact results when $\omega_L = 700$, only 3.5 times greater than the maximum,

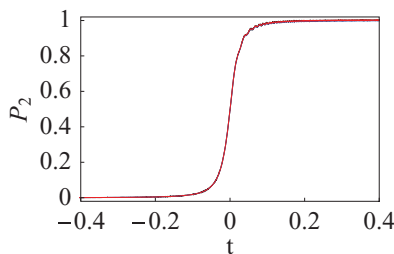


FIG. 3. (Color online) Population of the excited state for the exact dynamics and for the RWA approximations with the quadrature signal and the analytic signal. The carrier frequency is large enough so that the three lines essentially coincide. Parameters: $b = 3500$, $\mathcal{E}_0 = 200$, and $\omega_L = 20000$.

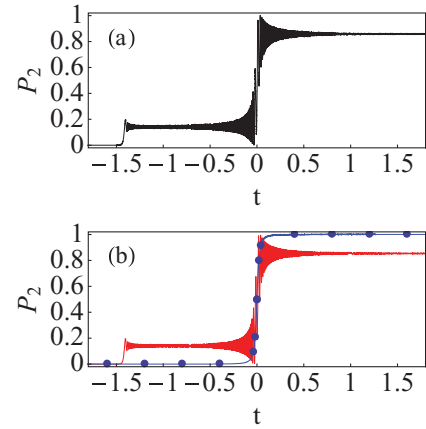


FIG. 4. (Color online) Population of the excited state for (a) the exact dynamics (b) the Hamiltonian in the RWA for the quadrature signal (blue line with dots) and the analytic signal (solid red line). Compare to the previous figure. As ω_L decreases, only the analytic signal RWA follows the exact dynamics. Parameters: $b = 3500$, $\mathcal{E}_0 = 200$, and $\omega_L = 5000$.

$\Omega_{Ra}(0) = 200.08$. For $\omega_L \approx 600$ (figure not shown), a small discrepancy appears between the populations of the exact and analytic RWA model which increases with decreasing ω_L .

There is, according to the construction of the pulse and the condition $\omega_L = \omega_0$, a resonance region at $t = 0$. The early excitation at negative times in Figs. 4 and 5 is due to the crossing of an additional resonance region where the instantaneous frequency becomes, in the quadrature model, $-\omega_0$, see Fig. 6. Using as before $\omega_0 = \omega_L$, we have that $\omega_L = |\omega_L + 2bt|$ has solutions $t = 0$, corresponding to the nominal resonance of the pulse, and also

$$t = t_r := -\omega_L/b. \quad (31)$$

As shown in Figs. 4 and 5, the quadrature RWA does not notice this “negative-frequency” (NF) resonance, since the negative instantaneous frequency corresponds in fact to a large quadrature detuning $\Delta_q = 2\omega_0$ at t_r . Instead, the instantaneous frequency for the analytic signal is positive at t_r and gives $\Delta_a = 0$, see Fig. 6. The condition for the NF resonance to

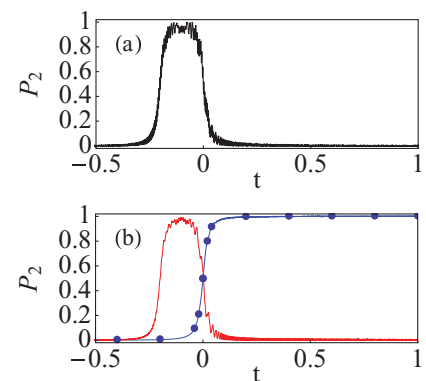


FIG. 5. (Color online) Population of the excited state for (a) exact dynamics; (b) RWA for the quadrature signal (blue line with dots) and the analytic signal (solid red line). Parameters: $b = 3500$, $\mathcal{E}_0 = 200$, $\omega_L = 700$.

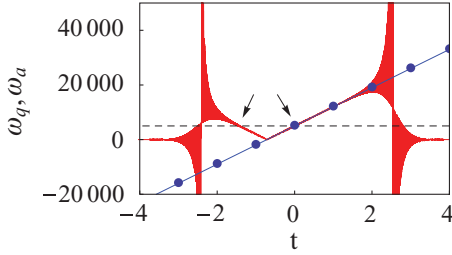


FIG. 6. (Color online) Instantaneous frequencies $\omega_q(t) = \omega_L + 2bt$ (blue line with dots) and $\omega_a(t)$ (solid red line). Parameters: $b = 3500$, $\mathcal{E}_0 = 200$, and $\omega_L = 5000$. The dashed line is at ω_L . The arrows indicate the early, and nominal resonance regions for the pulse, when $\omega_a = \omega_L$.

occur out of the pulse (therefore having no consequence) is that $|t_r| \gg 3\sigma_r$, i.e.,

$$\omega_L \gg 3b/2. \quad (32)$$

This is independent of the magnitude of the interaction. Since the difference between the single-resonance condition in Eq. (32) and the closeness condition in Eq. (29) is just a numerical factor, when $b \gg 1$, the separation of analytic and quadrature approximate RWA dynamics is associated with the occurrence of this early NF resonance within the pulse. Figure 7 depicts an example of an ultrachirped real signal capable of inducing a double resonance. The passage through zero instantaneous frequency is evident as a gap in the lower envelop and nearby slow oscillations.

The complete population return shown in Fig. 5 is stable for b between $b = 2000$ to $b = 4000$. Since varying b amounts to shifting the NF resonance, this provides “windows” of excitation of controllable duration, potentially useful for optical gating, with switching times much shorter than the pulse duration.

B. Adiabatic approximation

It is interesting to complement the above results by examining the validity of the adiabatic approximation. The condition for the states evolving with the Hamiltonians in Eqs. (23) and (25) to behave adiabatically following the instantaneous eigenstates is

$$|\Omega_d(t)| \gg \frac{1}{2} |\Omega_{Ad}(t)|, \quad (33)$$

where the subscript $d = q, a$ refers to the amplitude-phase decomposition, quadrature or analytic signal, $\Omega_d(t) = \sqrt{\Omega_{Rd}^2 + \Delta_d^2}$ is an effective Rabi frequency, the instantaneous energies for the Hamiltonians in Eqs. (23) and

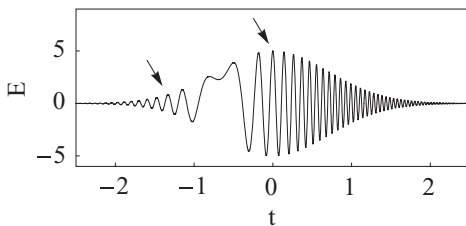


FIG. 7. Ultrachirped signal. The arrows indicate the resonance regions where $\omega_L = \omega_a$. Parameters: $b = 30$, $\mathcal{E}_0 = 5$, and $\omega_L = 40$.

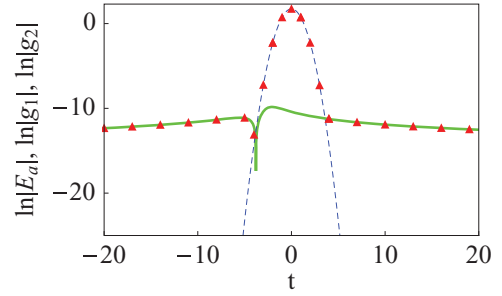


FIG. 8. (Color online) $\ln |E_a(t)|$ (red triangles) is essentially equal to $\ln |g_2(t)|$ (dashed blue line) in the central interval, and to $\ln |g_1(t)|$ (green solid line) in the asymptotic regions. Parameters: $b = 2$, $\mathcal{E}_0 = 4\sqrt{2}$, and $\omega_L = 10\sqrt{2}$.

(25) are $E_{d\pm}(t) = \pm\Omega_d(t)/2$, and $\Omega_{Ad}(t) = [\Omega_{Rd}\dot{\Delta}_d(t) - \Delta_d(t)\dot{\Omega}_{Rd}(t)]/\Omega_d^2(t)$.

In our numerical example, according to Eq. (29), $\omega_L = 20000$ is large enough to make the analytic and the quadrature signal models very similar. For this ω_L the adiabaticity condition is satisfied both for $E_q(t)$ and for $E_a(t)$. As we diminish ω_L , however, the adiabaticity condition is still satisfied for $E_q(t)$, but not for $E_a(t)$. This is quite evident, e.g., in Fig. 4, note the smooth curve of the quadrature signal model versus the coherent transients of the exact results or the analytic signal model [10,11].

III. DISCUSSION AND CONCLUSIONS

In this paper we have explored the consequences of going beyond common excitation regimes of a two-level quantum system, in particular we have seen that for ultrachirped fields the resonance condition may be satisfied twice, for positive and negative quadrature instantaneous frequencies along the linear chirp. The formal rotating wave approximation is more robust by using analytic signal theory for the complex signal and the corresponding interaction picture. The reason is that the analytic signal reinterprets the chirp, assigning positive frequencies to the pulse region with negative frequencies in the quadrature model. It may be conjectured that the analytic signal is the optimal choice with respect to the rotating wave approximation, as it tends to put the higher frequency components into the phase factor, but no proof exists.

Numerical examples demonstrate that the necessary dimensional parameters to see double resonances are within reach in the microwave domain with the current technology of pulse generators. A dimensional realization of the parameters of Fig. 5 could be as follows: $\omega_L = 2\pi \times 1.019$ GHz, $a = (2\pi)^2 \times 0.21 \times 10^{13}$ Hz², $b = (2\pi)^2 \times 7.4 \times 10^{15}$ Hz², which gives $\sigma_{tq} \approx 54$ ns, and $\sigma_{\omega q} \approx 2\pi \times 5.1$ GHz.

While this work has been essentially a curiosity-driven exploration, applications may be envisioned in state determination, optical gating and interferometry, since the timing of the resonance regions can be controlled. Specific fields we consider for future work are: circuit quantum electrodynamics, in which the two-level system and its interactions are highly tunable and potentially time dependent, and also cold atoms in counterpropagating laser beams inducing a Raman transition [12].

ACKNOWLEDGMENTS

We thank L. Cohen, I. Lizuain, R. Montero, and E. Solano for discussions. We acknowledge funding by the Basque Government (Grant No. IT472-10) and Ministerio de Ciencia e Innovación (FIS2009-12773-C02-01). S.I. acknowledges support from the Basque Government (Grant No. BF109.39).

APPENDIX: ASYMPTOTIC VALUES OF THE PHASE OF THE ANALYTIC SIGNAL

For a linearly chirped Gaussian pulse the phase $\theta_a(t) = \text{Im}[\ln E_a(t)]$ of the analytic signal (28) tends to a constant, see Fig. 2. $z = z(t) = t\sqrt{1-ib} - i\omega_L/(2\sqrt{1-ib})$ is a linear function of t , so as $|t|$ increases $z(t)$ becomes larger in modulus and asymptotic expressions of the w may be used. The asymptotic behavior of $E_a(t)$ for large $|z|$ and $\text{Im}[z(t)] > 0$ is

$$E_a(t) \sim \frac{\mathcal{E}_0}{2} \left[\frac{ie^{-\omega_L^2/4(1-ib)}}{\sqrt{\pi}z(t)} + \frac{ie^{-\omega_L^2/4(1+ib)}}{\sqrt{\pi}z^*(t)} + 2e^{-\omega_L^2/4(1+ib)}e^{-(z^*)^2(t)} \right], \quad (\text{A1})$$

whereas for $\text{Im}[z(t)] < 0$ [13],

$$E_a(t) \sim \frac{\mathcal{E}_0}{2} \left[\frac{ie^{-\omega_L^2/4(1-ib)}}{\sqrt{\pi}z(t)} + \frac{ie^{-\omega_L^2/4(1+ib)}}{\sqrt{\pi}z^*(t)} + 2e^{-\omega_L^2/4(1-ib)}e^{-z^2(t)} \right]. \quad (\text{A2})$$

Then,

$$\theta_a(t) \sim \arctan \left\{ \frac{F(t) \pm 2e^{-t^2} \sin[\theta_q(t)]}{2e^{-t^2} \cos[\theta_q(t)]} \right\} + 2\pi n, \quad (\text{A3})$$

where the negative and positive signs correspond to $\text{Im}(z) > 0$ and $\text{Im}(z) < 0$, respectively, $n = 0, 1, 2, \dots$ and

$$F(t) = \frac{2(1+b^2)^{1/4} [t \cos \alpha + (bt + \frac{\omega_L}{2}) \sin \alpha]}{\sqrt{\pi} [t^2 + (bt + \frac{\omega_L}{2})^2]} \times e^{-\omega_L^2/4(1+b^2)}, \quad (\text{A4})$$

with

$$\alpha = \frac{b\omega_L^2}{4(1+b^2)} + \frac{1}{2} \arctan b. \quad (\text{A5})$$

Independently of the signs \pm in Eq. (A3), when $t \rightarrow \pm\infty$, the argument of the arctangent tends to $+\infty$ or to $-\infty$. Therefore, the asymptotic expansion for the phase of the analytic signal will be

$$\theta_a(t) \sim \pm \frac{\pi}{2} + 2\pi n. \quad (\text{A6})$$

For $n = 0$, the phase remains inside the principal branch of the $\ln |E_a(t)|$, see Fig. 2. As the phase reaches these constant values, $\omega_a(t) \rightarrow 0$ when $t \rightarrow \pm\infty$.

To identify the transition between the central pulse and asymptotic regimes let us compare different terms with the full expression. Defining

$$g_1(t) = \frac{\mathcal{E}_0}{2} \left[\frac{ie^{-\omega_L^2/4(1-ib)}}{\sqrt{\pi}z(t)} + \frac{ie^{-\omega_L^2/4(1+ib)}}{\sqrt{\pi}z^*(t)} \right], \quad (\text{A7})$$

$$g_2(t) = \begin{cases} \mathcal{E}_0 e^{-\omega_L^2/4(1+ib)} e^{-(z^*)^2(t)} & \text{Im}[z(t)] > 0 \\ \mathcal{E}_0 e^{-\omega_L^2/4(1-ib)} e^{-z^2(t)} & \text{Im}[z(t)] < 0 \end{cases} \quad (\text{A8})$$

and comparing $\ln |E_a(t)|$ with $\ln |g_1(t)|$ and $\ln |g_2(t)|$, we see that (A8) dominates during the central interval, and (A7) in the outer time regions, see Fig. 8. Transition regions with interferences occur near the times when $\ln |g_1(t)|$ and $\ln |g_2(t)|$ are equal. For the parameters $b = 2$, $\mathcal{E}_0 = 4\sqrt{2}$, and $\omega_L = 10\sqrt{2}$, see Fig. 8, these instants are $t_1 = -3.862$ and $t_2 = 3.596$, so the pulse is essentially within the central interval, see Fig. 1.

-
- [1] C. Fleming, N. I. Cummings, C. Anastopoulos, and B. L. Hu, *J. Phys. A* **43**, 405304 (2010).
- [2] A. Messiah, *Quantum Mechanics* (North Holland, Amsterdam, 1961), Vol. 1.
- [3] C. Cohen-Tannoudji, B. Diu, and F. Laloë, *Quantum Mechanics* (Wiley-VCH, Berlin, 2005), Vol. 1.
- [4] X. Chen, I. Lizuain, A. Ruschhaupt, D. Guéry-Odelin, and J. G. Muga, *Phys. Rev. Lett.* **105**, 123003 (2010).
- [5] L. Cohen, *Time-frequency Analysis* (Prentice Hall PTR, Saddle River, NJ, 1995).
- [6] V. N. Faddeyeva and N. M. Terentev, *Mathematical Tables: Tables of the Values of the Function $w(z)$ for Complex Argument* (Pergamon, New York, 1961).
- [7] A. Abramowitz and I. A. Stegun, *Handbook of Mathematical Functions* (Dover, New York, 1965).
- [8] C. Cohen-Tannoudji, J. Dupont-Roc, and G. Grynberg, *Atom-Photon Interactions* (Wiley Interscience, New York, 1998).
- [9] L. Allen and J. H. Eberly, *Optical Resonance and Two-Level Atoms* (Wiley Interscience, New York, 1975).
- [10] S. Zamith, J. Degert, S. Stock, B. de Beauvoir, V. Blanchet, M. A. Bouchene, and B. Girard, *Phys. Rev. Lett.* **87**, 033001 (2001).
- [11] A. Monmayrant, B. Chatel, and B. Girard, *Phys. Rev. Lett.* **96**, 103002 (2006).
- [12] B. Chatel and B. Girard, in *Femtosecond Laser Spectroscopy*, edited by P. Hannaford (Springer, Boston, USA, 2005), Chap. 10.
- [13] J. G. Muga and M. Büttiker, *Phys. Rev. A* **62**, 023808 (2000).